Synthesis, Structure, and Properties of [Hg$_6$P$_4$](TiCl$_6$)Cl: The Problem of Host–Guest Interactions

Andrei V. Olenev and Andrei V. Shevelkov[1]

Inorganic Synthesis Laboratory, Department of Chemistry, Moscow State University, Moscow 119899, Russia

[Hg$_6$P$_4$](TiCl$_6$)Cl is synthesized in an ampoule at 400°C. Its crystal structure is solved on the basis of a CAD4 single-crystal experiment in a cubic space group *Pa*-3 (*a* = 11.7675(6) Å, *Z* = 4, *R* = 0.0331). The structure is comprised of the three-dimensional cationic framework $^3_\infty$[Hg$_6$P$_4$]$^{4+}$, and two different guest anions, octahedral TiCl$_6^{3-}$ and monoatomic Cl$^-$, trapped in the cavities of the host framework. The magnetic properties of the title compound reflect the presence of the Ti^{3+} (d^1) centers. The host–guest interaction in [Hg$_6$P$_4$](TiCl$_6$)Cl is discussed on the basis of the results of tight-binding band structure and molecular orbital calculations performed on the host framework and octahedral guest. © 2001 Academic Press

Key Words: host–guest compounds; extended frameworks; mercury pnictide halides; building units; crystal and electronic structure.

INTRODUCTION

Inorganic supramolecular chemistry often deals with complexes built of electrically charged hosts and guests (1). Such complexes are frequently obtained by high-temperature synthesis or under hydrothermal conditions, where the possibilities to study mechanisms, in particular the nature of intermediates, are very limited, if they exist at all. The majority of the products do not exhibit positional and/or rotational disorder of the guest ions trapped in the close cavities of the extended frameworks. This seems to indicate that the host–guest interaction, being much weaker than the covalent bonding within the hosts and guests, plays an important role in formation/assembling of complexes during synthesis, and, together with the geometry/topology requirements, provides the match between the hosts and guests.

Recently (2), we showed that the host–guest interactions in [Hg$_7$As$_4$I$_3$]SnI$_3$ cause a departure of the geometry of the guest anion SnI$_3^-$ from the equilibrium. In the present work

we deal with [Hg$_6$P$_4$](TiCl$_6$)Cl, a novel member of the family of phases based on the different cationic three-dimensional framework of the generic formula $^3_\infty$[M$_6$Z$_4$]$^{4+}$, where M = Cd, Hg; Z = P, As, Sb (3–8). This framework possesses closed cavities of two different sizes. Several examples of these phases are known. In some of them a trivalent cation, Ti^{3+}, Mo^{3+} (6), Sb^{3+}, Bi^{3+} (7), or In^{3+} (8), centers the octahedral guest, the excess charge being compensated by the halide anion, Cl$^-$ or Br$^-$. In the case of [Cd$_6$P$_4$]CdCl$_6$ (5) the smaller cavities are vacant, while in [Hg$_6$As$_4$](HgCl$_6$) Hg$_{0.4}$ (4) they are 40% occupied by mercury atoms, having an oxidation number 0 (9).

In this article we report the synthesis, structure, and properties of [Hg$_6$P$_4$](TiCl$_6$)Cl. Some aspects of its electronic structure are discussed in relation to the host–guest interaction.

EXPERIMENTAL SECTION

For the preparation of [Hg$_6$P$_4$](TiCl$_6$)Cl, mercury(I) chloride, titanium shavings (both > 99.9% purity), and red phosphorus (97%) were used as starting materials. Phosphorus was washed before use consecutively by a 30% aqueous solution of KOH, water, and ethanol (twice), and then vacuum-dried. The other reagents were used as received. The starting materials were mixed in a 7:2:8 molar ratio. The mixture (1 g total weight) was vacuum-sealed in a silica tube and annealed for 4 days at 400°C in a tube furnace. The sealed tube (length, 65 mm; inner diameter, 7 mm) was placed in the furnace vertically. The product appeared at the bottom of the tube as a black polycrystalline air-stable powder, dark-brown after grinding. The excess mercury deposited in the upper part of the tube. The X-ray powder diffraction pattern (FR 552 (Nonius) Guinier chamber, Cu$K\alpha_1$ radiation) showed no traces of starting materials or known ternary phases. All reflections were indexed in a cubic system with a unit cell edge $a = 11.7675(6)$ Å. The sample did not contain single crystals suitable for structural investigations. For a single-crystal preparation, starting materials were mixed in a molar ratio

[1] To whom correspondence should be addressed. Fax: (7-095) 9394788. E-mail: shev@inorg.chem.msu.ru.
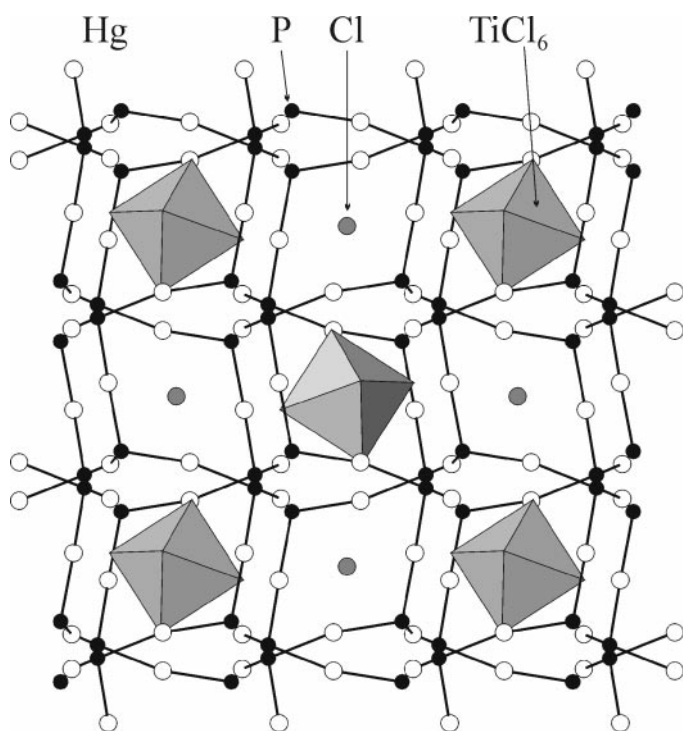
FIG. 1. Projection of the crystal structure of [Hg$_6$P$_4$](TiCl$_6$)Cl onto (001).

2:1:2 (1 g), vacuum-sealed in a silica ampoule, and annealed for 2 days at 500°C and then for 2 days at 300°C. After the furnace-cooling, the desired single crystals of different sizes and shapes were found all over the ampoule.

A black single crystal (0.25 × 0.2 × 0.2 mm^3) having an irregular shape was selected from the mixture and mounted on a CAD 4 (Nonius) goniometer head. The cubic unit cell parameter $a = 11.762(2)$ Å was refined on the basis of 24 well-centered reflections. The data were collected in the ω–2θ mode at ambient temperature with the data collection parameters listed in Table 1. A semi-empirical absorption correction was applied to the data on the basis of ψ-scans of five reflections having their χ angles close to 90°. Analysis of systematic absences pointed at the space group Pa-3 (No. 205). The positions of mercury and titanium atoms were localized by direct methods (SHELXS 97 (10)). Phosphorus and chlorine atoms were found from a sequence of $\Delta\rho(xyz)$ syntheses and least-squares cycles (SHELXL 97 (11)). Final anisotropic refinement against F^2 led to $R_1 = 0.0331$.

Atomic coordinates and equivalent thermal displacement parameters are listed in Table 2; bond lengths and valence angles are summarized in Table 3. Further details of the crystal structure determination may be obtained from Fachinformationszentrum Karlsruhe, D-76344 Eggenstein-Leopoldshafen, Germany, on quoting the depository number CSD-411415.

Magnetic susceptibility measurements were performed in the temperature range of 104–295 K exploiting a standard Faraday balance technique. The sample was first checked for monophasity with the help of a profile analysis of an X-ray diffractogram (STADI-P (STOE), Cu$K\alpha_1$ radiation). After correction for a Langevin term, the magnetic moment was found to be 1.8(1) μ_B. Only a very slight increase of the magnetic moment was found on going from 104 to 295 K, the value difference being within the range of the experimental errors.

An ESR spectrum was recorded at room temperature on an EMX 1104 (Brucker) spectrometer operated at 9.5 GHz. The sample was checked for monophasity as described above.

Computational Aspects

Tight-binding extended Hückel band structure calculations (12) were carried out on the $^3_\infty$[Hg$_6$P$_4$]$^{4+}$ cationic framework having the geometry found from the crystal structure analysis. The same type of molecular orbital calculations were performed on the TiCl$_6^{3-}$ anion having O_h symmetry, d(Ti–Cl) = 2.42 Å. The PC versions (13, 14) of the programs developed by Hoffman's group at Cornell University were used. Implemented in these programs were atomic orbital parameters for mercury, phosphorus, and chlorine; those for titanium are taken from Ref. (15).

RESULTS AND DISCUSSION

[Hg$_6$P$_4$](TiCl$_6$)Cl was prepared not by a stoichiometric synthesis but according to the reaction

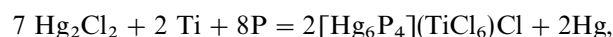$$7 \text{ Hg}_2\text{Cl}_2 + 2 \text{ Ti} + 8\text{P} = 2[\text{Hg}_6\text{P}_4](\text{TiCl}_6)\text{Cl} + 2\text{Hg},$$

TABLE 1
Data Collection and Structure Refinement Parameters for [Hg$_6$P$_4$](TiCl$_6$)Cl

Space group	Pa-3
Cell parameter a (Å)^a	11.7675(6)
V (Å^3)	1627.2(5)
Z	4
Density (calc) (g cm^{-3})	6.627
Radiation, λ, (Å)	Mo $K\alpha$, 0.71069
μ (mm^{-1})	58.369
Data collection range (deg)	$3.00 < \theta < 25.96$
Reflections collected	1607
Independent reflections	543 [R(int) = 0.0744]
Parameters refined	30
R_1,^{b} wR_2^{c} ($F_o > 4\sigma F_o$)	0.0331, 0.0604
R_1, wR_2 (all data)	0.0547, 0.0636
Largest diff peak and hole (e/Å^3)	1.848 and $-$1.585
GOF on F^2	1.034

^{a} Guinier data. $^b R_1 = \sum \|F_o| - |F_c\|/\sum |F_o|$. ^{c} w$R_2 = [\sum w(F_o^2 - F_c^2)^2/ \sum w(F_o^2)^2]^{1/2}$, $w = [\sigma^2(F_o^2) + 0.0199 (F_o^2 + 2F_c^2)/3]^{-1}$.

TABLE 2
Atomic Coordinates and Equivalent Thermal Displacement Parameters for $[Hg_6P_4](TiCl_6)Cl$

Atom	Wykoff	x/a	y/b	z/c	$U_{(eq)}$[a]
Hg	24d	0.3009(1)	0.0398(1)	0.6935(1)	0.0119(2)
P(1)	8c	0.1613(3)	0.1613(3)	0.1613(3)	0.005(1)
P(2)	8c	0.7307(3)	0.7307(3)	0.7307(3)	0.004(1)
Ti	4b	0	0	$\frac{1}{2}$	0.006(1)
Cl(1)	24d	0.9544(3)	0.1964(3)	0.4599(3)	0.0107(6)
Cl(2)	4a	$\frac{1}{2}$	0	$\frac{1}{2}$	0.036(2)

[a] U_{eq} is defined as one-third of the trace of the orthogonalized U_{ij} tensor.

which was carried out at 400°C. Under these conditions a complete separation of the products was achieved. The target compound resided at the bottom of the ampoule, while tiny drops of mercury were "glued" to the silica walls at the upper part of the ampoule. Visual analysis of the product under a ×28 microscope confirmed the absence of unreacted mercury and phosphorus in the solid product. The absence of crystalline admixtures was confirmed by the X-ray analysis (Guinier). The accuracy of the latter gives the appreciated 99.5% purity of the target phase.

The crystal structure of $[Hg_6P_4](TiCl_6)Cl$ is comprised of an extended cationic framework $^3_\infty[Hg_6P_4]^{4+}$ and two guest anions, $TiCl_6^{3-}$ and Cl^-, trapped in cavities of two different sizes (Fig. 1). The mercury atom is connected to two phosphorus atoms and has a P–Hg–P angle of 167.5°. Two crystallographically independent phosphorus atoms have similar, almost regular tetrahedral arrangements built of one phosphorus atom and three mercury atoms. Thus formed the P–P dumbbell is octahedrally surrounded by six mercury atoms. Such octahedra share all vertices to form a perovskite-like framework. The P–P bond distance of

TABLE 3
Selected Bond Lengths and Valence Angles for $[Hg_6P_4](TiCl_6)Cl$

Bond Lengths/Å	
P(1)–Hg	2.436(3) (×3)
P(2)–Hg	2.444(3) (×3)
P(1)–P(2)	2.203(9)
Ti–Cl(1)	2.418(4) (×6)
Angles/deg	
P(1)–Hg–P(2)	167.5(1)
P(2)–P(1)–Hg	111.4(1) (×3)
Hg–P(1)–Hg	107.4(1) (×3)
P(1)–P(2)–Hg	114.0(1) (×3)
Hg–P(2)–Hg	104.6(1) (×3)
Cl(1)–Ti–Cl(1)	180 (×3)
Cl(1)–Ti–Cl(1)	89.0(1) (×6)
Cl(1)–Ti–Cl(1)	91.0(1) (×6)

2.20 Å found in the 3D framework is typical for compounds containing P_2^{4-} units, where such separations lie in the range of 2.19–2.21 Å (5, 16–18), and is characteristic of a single bond (19). The Hg–P distances (all 2.44 Å) are also usual for mercury phosphide halides (16, 17, 20, 21).

There are two types of cavities in the host framework. The smaller cavities are centered with the 4a position, and the larger ones with the 4b position of the space group Pa-3. The smaller cavities are occupied by the $Cl(2)^-$ anions, while in the larger cavities the octahedral anions $TiCl(1)_6^{3-}$ are situated. Coordination of the titanium atom is very close to regular octahedral (Table 2); all six bonds are the same, while maximum deviation of the Cl–Ti–Cl angles from the ideal values is only 1°. The Ti–Cl(1) distances of 2.42 Å are in good correspondence with the values found for numerous Ti^{3+}-containing compounds. For example, in different crystalline modifications of $TiCl_3$ the Ti–Cl separations cover the range from 2.33 to 2.50 Å (22). The shortest host–guest distances, i.e., the Hg–Cl(1) and Hg–Cl(2) distances, are 3.07 and 3.30 Å, respectively, which is much longer than the covalent bond lengths found in $HgCl_2$ (2.27–2.29 Å) (23).

Some other examples of compounds with the same structural organization have been reported: $[Hg_6As_4](TiBr_6)Br$, $[Hg_6As_4](TiCl_6)Cl$, $[Hg_6As_4](MoCl_6)Cl$ (6), $[Hg_6As_4](BiCl_6)Cl$, $[Hg_6Sb_4](SbBr_6)Br$, $[Hg_6As_4](BiBr_6)Br$ (7), $[Hg_6As_4](InCl_6)Cl$ (8), $[Hg_6As_4](HgCl_6)Hg_{0.4}$ (6), and $[Cd_6P_4](CdCl_6)$ (5). While the first seven compounds are full analogues of $[Hg_6P_4](TiCl_6)Cl$, the last two have certain structural differences from the title compound. The structure of the host framework is the same in all nine phases. But in the case of the compounds containing titanium, indium, and molybdenum, the smaller cavities are filled by Cl^- or Br^- anions, while in $[Hg_6As_4](HgCl_6)Hg_{0.4}$ they are 40% occupied by zero-valence mercury atoms, and remain empty in $[Cd_6P_4](CdCl_6)$. Noticeably, only halogen atoms, which serve as the monoatomic guests, fully (100%) occupy the smaller cavities. Evidently, the full population of the sites by the X^- anions is necessary to achieve electroneutrality. It is not clear, however, why the occupancy of the site is partial or zero when the charge is balanced by the MX_6^{4-} anions. So far we have no explanation for this fact.

The distribution of the guest anions in the title compound is the same as that in the phases containing the trivalent transition metal (6, 7). The oxidation state +3 for titanium parallels the observed magnetic properties of $[Hg_6P_4](TiCl_6)Cl$, where the spin-only moment of $3^{1/2} \approx 1.73$ mB, due to the d^1 Ti^{3+} center, is expected. In a recent article (6), Beck and Neisel have showed that magnetic behavior of the analogous Ti-containing phases $[Hg_6As_4](TiCl_6)Cl$ and $[Hg_6As_4](TiBr_6)Br$ is best described on the basis of a spin–orbital coupling, resulting in a certain increase of the magnetic moment with increasing temperature. It should be mentioned that the model used by Beck and Neisel implies a complete separation of the guest anions ($TiCl_6^{3-}$) from

TABLE 4
Host–Guest Distances in [Hg$_6$Z$_4$](TiX$_6$)X (Z = P, As; X = Cl, Br) Compared to Short and Long Hg–X Separations in the Respective Mercury Dihalides (Å)

Compound	X(1)–Hg	X(2)–Hg	Short in HgX$_2$	Long in HgX$_2$
[Hg$_6$P$_4$](TiCl$_6$)Cl	3.07 (×2)		Cl–Hg[b]	Cl–Hg[b]
	3.10	3.30 (×6)	2.27–2.29	3.38–3.46
	3.21			
[Hg$_6$As$_4$](TiCl$_6$)Cl[a]	3.13	3.35 (×6)	Cl–Hg[b]	Cl–Hg[b]
	3.16		2.27–2.29	3.38–3.46
	3.23			
	3.26			
[Hg$_6$As$_4$](TiBr$_6$)Br[a]	3.20 (×2)	3.44 (×6)	Br–Hg[c]	Br–Hg[c]
	3.24		2.46	3.23
	3.36			

[a] From Ref. (6). [b] From Ref. (23). [c] From Ref. (24).

each other, which is evident, as well as from the hosting framework, which is not so apparent. Table 4 summarizes the host–guest Hg–X distances in all three Ti-containing

compounds. It is clear that the separation between the mercury atoms of the framework and the halogen atom of the TiX$_6^{3-}$ anion is significantly larger than in the respective binary halides (23, 24), but still too short to neglect the (noncovalent) interactions between host and guest substructures.

To shed some light on the nature of the host–guest interactions, we performed the extended Hückel calculations (12) of the electronic structure of [Hg$_6$P$_4$](TiCl$_6$)Cl. It was clear from the crystal structure alone that strong bonding is expected within the host framework and within the guest anion. Therefore, we performed band structure calculations on the host $^3_\infty$[Hg$_6$P$_4$]$^{4+}$ framework, and molecular orbital calculations on the guest (TiCl$_6$)$^{3-}$ anion, and then compared the results on a common energy scale. In such a way we avoided overestimating the Hg–Cl host–guest orbital interaction. We also neglected the contribution of the smaller guest, Cl$^-$, due to its evident closed-shell nature with low-lying orbitals. The results of the calculations are shown in Fig. 2.

The principal building unit of the $^3_\infty$[Hg$_6$P$_4$]$^{4+}$ framework is the (Hg$_6$P$_2$) octahedron. Recently (17), we examined the electronic structure of the model cation (Hg$_6$P$_2$)$^{8+}$. We
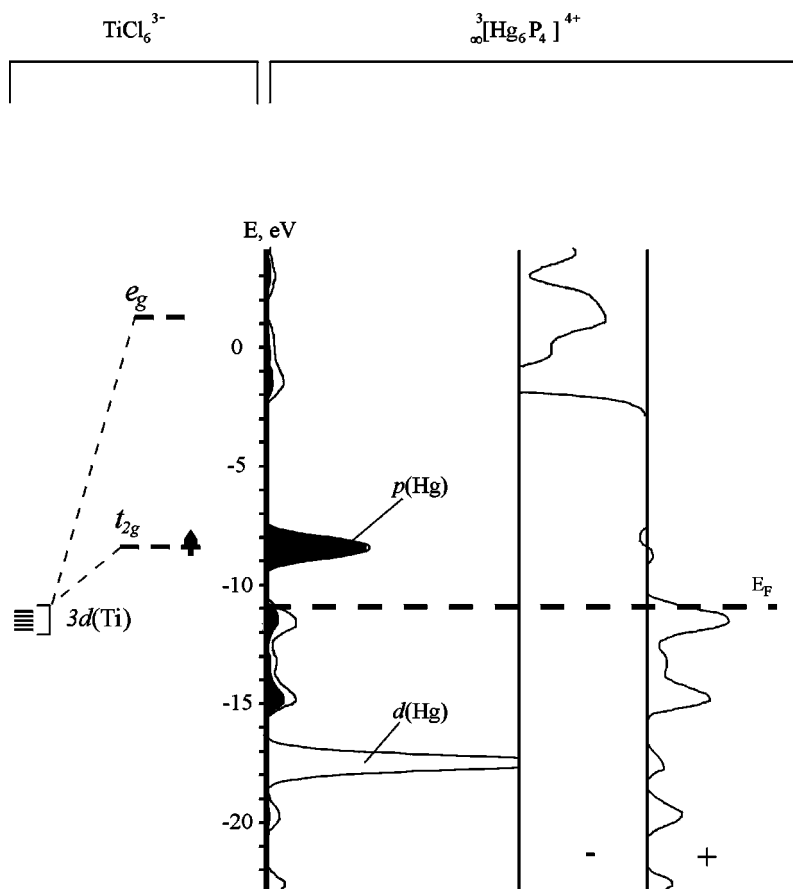

FIG. 2. Charge-transfer scheme from the extended Hückel calculations. Left: MO for the TiCl$_6^{3-}$ anion; the 3d level of Ti is given for comparison. Center: Total DOS curve for [Hg$_6$P$_4$]$^{4+}$; s and p contributions of Hg are shaded. Right: COOP curve for the Hg–P interaction in [Hg$_6$P$_4$]$^{4+}$.

have shown, in particular, that the HOMO and the orbitals just below are composed mainly of the π^*, π, and σ_z orbitals of the P_2^{4-} unit, which interact strongly with the s orbitals of six mercury atoms, but a certain admixture of the Hg d orbitals was also found. Figure 2 shows that after condensation of the octahedra into the $^3_\infty[Hg_6P_4]^{4+}$ framework, the states just below the Fermi level retain their nature, the contribution of phosphorus p orbitals and mercury s orbitals being dominant. More important is that the nonbonding Hg p orbitals, upon condensation of the octahedra, form the rather narrow band lying above the Fermi level but below the continuum. The Hg partial DOS (density of states) and Hg–P COOP (crystal orbital overlap population) confirm that this band is composed predominantly of the nonbonding Hg p orbitals, and can act as an intrinsic acceptor band. Comparison with the MO diagram of the $TiCl_6^{3-}$ anion makes it evident that the t_{2g} level has about the same energy as the acceptor band. It is clear from drawings that the t_{2g} MOs of $TiCl_6^{3-}$ are not nonbonding but rather Ti–Cl π antibonding, and they are not localized on the Ti atom. Consequently, the t_{2g} level can provide its single electron to the acceptor band, and this can be an indicator of the nature of the host–guest interaction.

The above-described electronic structure of $[Hg_6P_4]$ $(TiCl_6)Cl$ gives a model of the host–guest charge transfer. Still it is only a model, a rough, but plausible one. We can add some evidence in support, too. While the bulk properties of the title compound, and those described by Beck and Neisel (6), are consistent with the d^1 description (magnetic behavior, for example, as shown above), our preliminary ESR data are in contradiction with the presence of the localized d^1 centers. The ESR spectrum of $[Hg_6P_4]$ $(TiCl_6)Cl$ recorded at room temperature exhibits a rather sharp signal with a g-factor equal to 2.0054, which is just above the g-factor of a "free" electron (2.0023). If the constant of the spin–orbital coupling were equal to 155 cm^{-1}, as applied by Beck and Neisel to model the dependence of the magnetic moment upon temperature for the Ti^{3+}-containing phases, the ESR spectrum would not be observed at all. That is typical for octahedral complexes of Ti(III) (25). The systematic study of the analogues of the title compound, mainly by means of NMR, ESR, and Mössbauer spectroscopy, is currently underway.

ACKNOWLEDGMENTS

REFERENCES

1. A. Müller, H. Reuter, and S. Dillinger, *Angew. Chem.* **107**, 2505–2539 (1995); *Angew. Chem., Int. Ed. Engl.* **34**, 2328–2361 (1995).
2. A. V. Olenev, A. I. Baranov, A. V. Shevelkov, and B. A. Popovkin, *Eur. J. Inorg. Chem.* **2000**, 265–270 (2000).
3. A. V. Shevelkov, E. V. Dikarev, and B. A. Popovkin, *J. Solid State Chem.* **98**, 133–136 (1992).
4. A. V. Shevelkov, E. V. Dikarev, and B. A. Popovkin, *J. Solid State Chem.* **126**, 324–327 (1996).
5. A. V. Shevelkov, L. N. Reshetova, and B. A. Popovkin, *J. Solid State Chem.* **137**, 138–142 (1998).
6. J. Beck and U. Neisel, *Z. Anorg. Allg. Chem.* **626**, 1620–1626 (2000).
7. J. Beck, S. Heddereich, and U. Neisel, *J. Solid State Chem.* **154**, 350–355 (2000).
8. A. V. Olenev and A. V. Shevelkov, "Book of Abstracts," 2nd National Crystallochemical Meeting, May 22–26, 2000, Chernogolovka, Russia, p. 9, 2000.
9. A. V. Shevelkov, "Book of Abstract," 6th European Conference on Solid State Chemistry, September 17–20, 1997, Zürich, Switzerland, Vol. I, p. ML7, 1997.
10. G. M. Sheldrik, SHELXS-97, program for crystal structure solution, University of Göttingen, Germany, 1997.
11. G. M. Sheldrik, SHELXL-97, program for crystal structure refinement, University of Göttingen, Germany, 1997.
12. J. H. Ammeter, H. B. Bürgi, J. C. Thibeaut, and R. Hoffmann, *J. Am. Chem. Soc.* **100**, 3686 (1978).
13. C. Mealli and D. M. Proserpio, *J. Chem. Educ.* **67**, 3399–3402 (1990).
14. M. Brändle, R. Rytz, and G. Calzaferri, BICON-CEDiT, manual. University of Bern, Switzerland, 1997.
15. P. Pyykkö and L. L. Lohr, Jr., *Inorg. Chem.* **20**, 1950 (1981).
16. A. V. Shevelkov, E. V. Dikarev, and B. A. Popovkin, *J. Solid State Chem.* **104**, 177–180 (1993).
17. A. V. Olenev, A. V. Shevelkov, and B. A. Popovkin. *J. Solid State Chem.* **142**, 14–18 (1999).
18. A. Rebbah and A. Deschanvres, *Rev. Chim. Mineral.* **18**, 125–132 (1981).
19. H. G. von Schnering and W. Hönle, *Chem. Rev.* **88**, 243–273 (1988).
20. M. Ledesert, A. Rebbah, and Ph. Labbe, *Z. Kristallogr.* **192**, 223–226 (1990).
21. A. V. Shevelkov, E. V. Dikarev, and B. A. Popovkin, *Z. Kristallogr.* **209**, 583–585 (1994).
22. S. I. Troyanov, E. M. Snigireva, and V. B. Rybakov, *Zh. Neorg. Khim.* **36**, 1117–1122 (1991).
23. V. Subramanian and K. Seff, *Acta Crystallogr. B* **36**, 2132–2135 (1980).
24. V. I. Pakhomov, A. V. Goryunov, I. N. Ivanova-Korfini, A. A. Boguslavskii, and R. S. Lotfullin, *Zh. Neorg. Khim.* **35**, 2476–2478 (1990).
25. R. S. Drago, "Physical Methods in Chemistry," Chapter 13. Saunders, Philadelphia, 1977.